IL NUOVO CIMENTO Vol. 35 C, N. 5 Settembre-Ottobre 2012
DOI 10.1393/ncc/i2012-11326-2

Communications: SIF Congress 2011

Toward ghost imaging with cosmic ray muons

M. D'Angelo(*)

Dipartimento Interateneo di Fisica, Università di Bari and INFN, Sezione di Bari - Bari, Italy

ricevuto il 31 Dicembre 2011; approvato il 13 Marzo 2012

Summary. — Optical ghost imaging exploits the correlation between two light beams to reproduce the image of a remote object without employing imaging optics or high-resolution detectors near the object. In this paper we propose and investigate the implementation of the ghost imaging protocol using correlated massive particles, namely, muons from cosmic ray air showers. The project Extreme Energy Events (EEE) offers a platform to study the feasibility of ghost imaging with such naturally available massive particles. Our analysis is based on coincidence detection between two neighbor schools of L'Aquila, where EEE muon telescopes operate. The observed coincidences show spatio-temporal correlations indicating the potentialities of this naturally available source for practical applications such as remote sensing. The demonstration of ghost imaging with massive particles will pave the way for the extension to particles of many other intriguing quantum optical phenomena involving classical and non-classical correlations.

PACS 03.65.Ud – Entanglement and quantum nonlocality.
PACS 42.50.-p – Quantum optics.
PACS 42.68.Sq – Image transmission and formation.
PACS 95.85.Ry – Neutrino, muon, pion, and other elementary particles; cosmic rays.

1. – Introduction

Optical ghost imaging is a technique that aims at gathering information on a distant object without the necessity of employing imaging optics or high-resolution detectors near the object [1-4]. This is achieved by using two correlated beams of light: One (probe) interacts with the distant object and is revealed by a "bucket" detector, with no spatial resolution; the other (reference), in a local laboratory, goes through imaging optics and is detected by a high spatial resolution detector. The correlation between

(*) E-mail: dangelo@fisica.uniba.it

the two beams allows revealing the structure of the object, remotely, from a coincidence measurement between the two detectors. Due to this property, optical ghost imaging has recently emerged as a promising low-light-level remote sensing tool [5-7].

Our group has recently proposed to investigate the feasibility of ghost imaging with correlated massive particles instead of light beams. Our leading idea is that muons generated by cosmic rays are an interesting source to study in the context of ghost imaging: As naturally available deeply penetrating particles characterized by an extremely small De Broglie wavelength, they are promising candidates for long distance high resolution ghost imaging.

The project Extreme Energy Events (EEE) [8] offers a platform for studying the feasibility of ghost imaging with cosmic ray muons. Muon "telescopes" composed of three Multigap Resistive Plate Chambers (MRPC) [9, 10], have been built and installed in many high schools across Italy. Some of them are already in operation and coincidence detection between muons have been measured in two neighbor schools of L'Aquila, 180 m apart [11,12]. Our analysis is based on the experimental data taken for 9 days in L'Aquila.

In this paper, we start with a brief review of quantum imaging, by introducing the ghost imaging experiments based on both entangled [1, 2] and separable systems of photons [13-17], as well as the ones based on chaotic light [3, 4, 18-22]. After introducing the EEE muon telescopes and the coincidence data collected in L'Aquila [11, 12], we present our analysis aiming at the extension of quantum imaging schemes to cosmic ray muons. In particular, after studying the spatio-temporal correlation characterizing the detected muon pairs, we present preliminary steps aiming at understanding the feasibility of muon ghost imaging and the related potentialities of this naturally available source for practical applications such as remote sensing.

The present work is the result of the collaboration of the Author with several researchers: G. Scarcelli (Harvard Medical School, Boston-MA), is the inventor of the present research activity, F. Di Lena (Physics Department, University of Bari) is the main developer of the data analysis presented here, under the supervision of A. Regano (Museo Storico della Fisica, Centro Studi e Ricerche E. Fermi, Roma), A. Garuccio and F. Romano (Physics Department of the University and Politecnico of Bari), as well as the Author [23]; M. D'Incecco (INFN LNGS, Assergi (AQ)) and R. Moro (Museo Storico della Fisica, Centro Studi e Ricerche E. Fermi, Roma) gave us the data here analyzed. The presented results represent a review of our recent work, namely, the first analysis of ghost imaging with massive particles; this represents an important step toward the extension to massive particles of many other intriguing quantum optical phenomena involving classical and non-classical correlations. From a practical standpoint, the natural abundance of cosmic ray muons on earth, their long-range correlation, extremely small De Broglie wavelength and high penetrating ability would suggest this protocol as a viable way to perform very long-distance high-resolution remote imaging.

2. – Review of optical ghost imaging

The first ghost imaging experiment was realized in the mid 1990s [2], following the theoretical proposal reported in ref. [1]. By exploiting the spatio-temporal entanglement characterizing signal-idler photon pairs emitted by Spontaneous Parametric Down-Conversion (SPDC) [24], Pittman *et al.* [2] demonstrated the possibility of reproducing the ghost image of an object, remotely: A mask (object) is inserted in front of a bucket detector, which simply counts the signal photons transmitted by the object; the idler photons propagate through an imaging lens and are detected by a distant photon counting

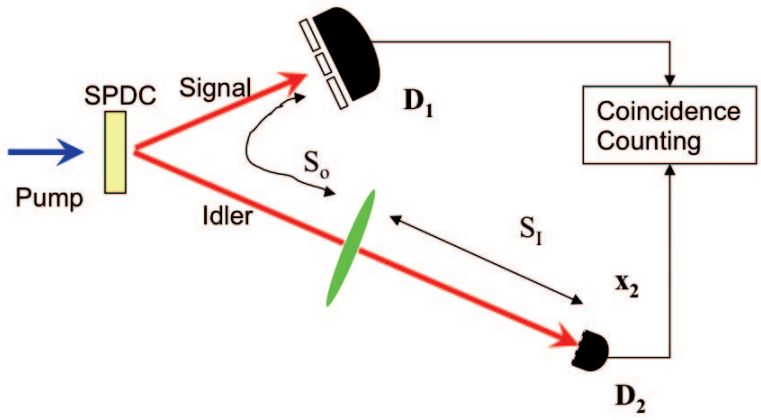

Fig. 1. – Schematic representation of the experimental set-up to observe ghost imaging with SPDC photon pairs: The object is illuminated by the signal photons only, while the idlers propagate through the imaging lens; a ghost image appears when counting coincidences between the fixed bucket detector D_1, placed behind the object, and the scanning point-like detector D_2, placed in the "ghost" image plane as defined by the Gaussian two-photon thin lens equation.

high resolution detector (fig. 1). The single counting rates at both detectors are always fairly constant.

The image of the mask is retrieved by recording the joint detection events of the signal-idler pairs while scanning the high-resolution detector in the two-photon image plane, as defined by the two-photon Gaussian thin lens equation:

$$\frac{1}{s_o} + \frac{1}{s_i} = \frac{1}{f}\,, \tag{1}$$

where f is the focal length of the lens, s_i is the lens-image distance, and s_o is the "ghost" object-lens distance, given by the sum of the distances from the object to the source (*i.e.*, the SPDC crystal) and from the source to the lens, as shown in fig. 1.

The experimental work by Bennink *et al.* [17] raised the question whether or not ghost imaging could be reproduced by classically correlated beams of light, as opposed to entangled photon pairs. The experimental set-up employed in this work is reported in fig. 2: Pairs of light beams classically correlated in momentum are focused by two separate lenses, the object is inserted in the focal plane of one lens, and coincidence counts are recorded between a bucket detector behind the object and a high-resolution detector placed in the focal plane of the other lens.

An intense debate was opened [13-16,25], as summarized in ref. [20]. One of the most interesting results that came out of this discussion is the possibility of producing ghost images by replacing the SPDC source with chaotic/thermal radiation [3, 4]: Similar to the entangled two-photon case, a two-photon Gaussian thin lens equation was found for this source [4]; the experimental set-up is shown in fig. 3. This effect is based on the spatio-temporal correlation first descoverd by Hanbury-Brown and Twiss (HBT) in the far field of a chaotic source [26]. However, the existence of a two-photon Gaussian thin lens equation for chaotic light indicates that such correlations are maintained also in the near field; in fact, chaotic ghost imaging was shown to exist not only when employing

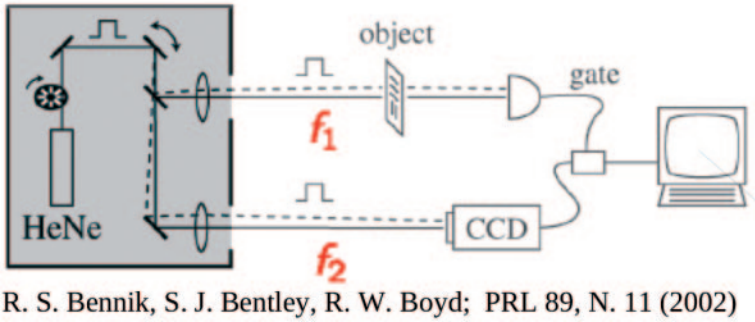

Fig. 2. – Experimental set-up of ref. [17] for simulating ghost imaging with two light beams classically correlated in momentum; the focal planes of the two lenses are required to transform the momentum correlation into the required "position" correlation.

an imaging lens, but also in a lens-less set-up, provided the object-source distance is exactly equal to the image-source distance [21, 22]. The effect is interpreted as the result of interference between indistinguishable two-photon events/alternatives. Beside the different two-photon thin lens equation, the most evident difference between chaotic light and entangled two-photon is the existence of a constant background noise accompanying the ghost image.

Beside its fundamental interest, quantum imaging has inspired several practical applications, from metrology [27] to low-light-level remote sensing [5-7].

3. – EEE muon telescopes

The Extreme Energy Events (EEE) Project [8] aims at studying the extremely high energy cosmic rays by means of muon detectors (also called telescopes) distributed over an area of about $10^6\,\mathrm{km}^2$, in Italy. In fact, the goal is to detect the muon component of Extensive Air Showers (EAS) by measuring coincidence events between distant telescopes. Each telescope consists of three 50 cm apart Multigap Resistive Plate Chamber (MRPC) [9], with an active area of about $2\,\mathrm{m}^2$, characterized by both time and position resolution, as well as tracking capability. As described in ref. [12], the electric signal generated by the passage of a particle through the detector is collected by one of the 24

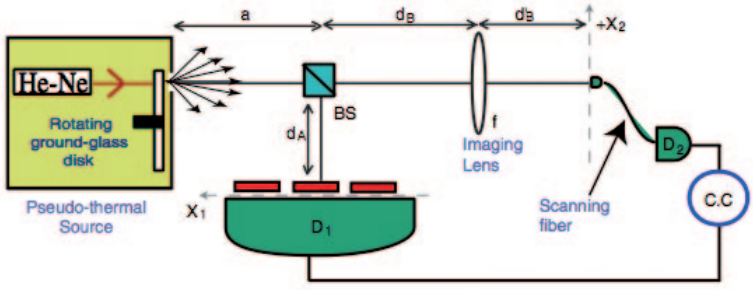

Fig. 3. – Experimental set-up employed in ref. [4] for observing ghost imaging with chaotic light, with $s_o = d_B - d_A$ and $s_i = d'_B$.

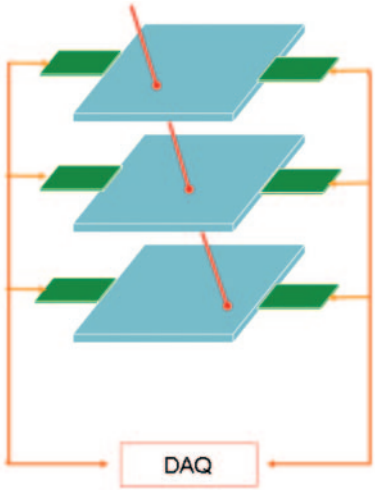

Fig. 4. – Sketch of the telescope employed in the EEE project. Each plane represents a MRPC; the hit points on the MRPCs allow reconstructing the track of the detected muon.

pick-up electrodes (160 cm-long copper strips with a pitch of 3.2 cm) mounted on each MRPC. The MRPC efficiency is around 95% and the time resolution is about 100 ps; the absolute time is recorded by a GPS, whose resolution is around 60 ns ($\sim \sqrt{2}\ \sigma_{\mathrm{GPS}}$). The hit strip and the difference between the signal arrival times at the strip ends enable reconstruction of the particle impact point (*i.e.*, its x-y coordinates), with a spatial resolution of about 2 cm [28]. The signals detected by each MRPC are collected only when a triple coincidence of the MRPCs occurs; a triple coincidence event in the telescope thus identifies the track of the detected particle, as shown in fig. 4. Data processing allows reconstructing the muon direction with an angular resolution of about 2° [28]; the acceptance of the EEE telescopes is 39° in the plane perpendicular to the copper strips and 58° in the orthogonal direction.

The present paper is based on the data taken for 9 effective days by two telescopes installed in two neighbor High Schools in L'Aquila, 180 m apart [11, 12], which we shall indicate as station A and B. In this paper we only consider the events where only a single track is present in each telescope, namely, we consider muon pairs detected at stations A and B, separately.

4. – Recent progresses toward muon ghost imaging

At the heart of optical ghost imaging is the temporal correlation between either photon pairs or light beams; the coincidence detection between distant photon/beams enables exploiting such temporal correlation. Either angular or momentum correlation is also required for guarantying the position correlation implicit in ghost images.

In order to study the feasibility of muon ghost images, we thus start by analyzing the temporal correlation between muons detected at stations A and B. The histogram of the time differences $(t_A - t_B)$ between muons detected by the two telescopes is characterized by a constant background and a peak centered around $t_A - t_B = 0$, as shown in fig. 5. The Gaussian fit $a \exp[-(x-\mu)^2/2\sigma^2] + b$ of the experimental data gives a peak visibility

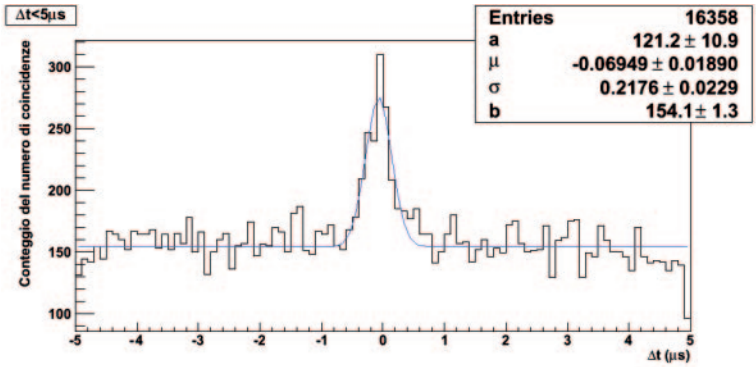

Fig. 5. – Temporal distribution of the muon pairs detected at stations A and B; Δt is the "corrected" detection time difference.

of 28% and a peak width of 220 ns. These results are in agreement with those presented in refs. [11, 12]. In fact, both the peak width and the constant background have been optimized by correcting the time differences for the average inclination ($\theta' = (\theta_A + \theta_B)/2$) of the detected muon pairs with respect to the line joining the two telescopes (having length L); the correction is implemented by replacing the detection time differences $t_A - t_B$ by [11, 12]: $\Delta t = t_A - t_B \pm L\cos(\theta')/c$.

Interestingly, a higher visibility peak ($V = 93\%$) is obtained by selecting the events characterized by almost parallel muon tracks, namely, having $\alpha < 5°$ where α is the angle between muons detected at the two stations (fig. 6). Such parallel track condition also gives a narrower peak width: $\sigma = 180$ ns.

The highly improved visibility of this new temporal peak indicates the existence of a strong angular correlation between the detected muon pairs. In addition, this result indicates that the nature of the observed correlation is certainly not predominantly chaotic; in fact, chaotic identical muons propagating in the same spatial mode (such as the one selected by imposing $\alpha < 5°$) would produce a fermionic HBT-type dip in the temporal histogram.

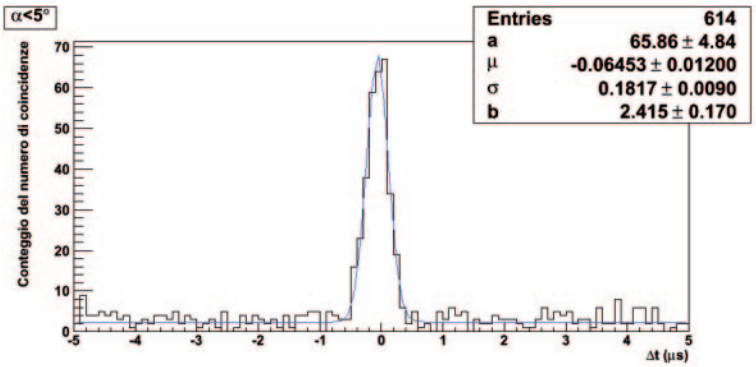

Fig. 6. – Temporal distribution of parallel muons detected at stations A and B: Δt is the "corrected" detection time difference; the condition of parallel tracks is imposed by selecting the angle between the tracks (α) to be smaller than 5°.

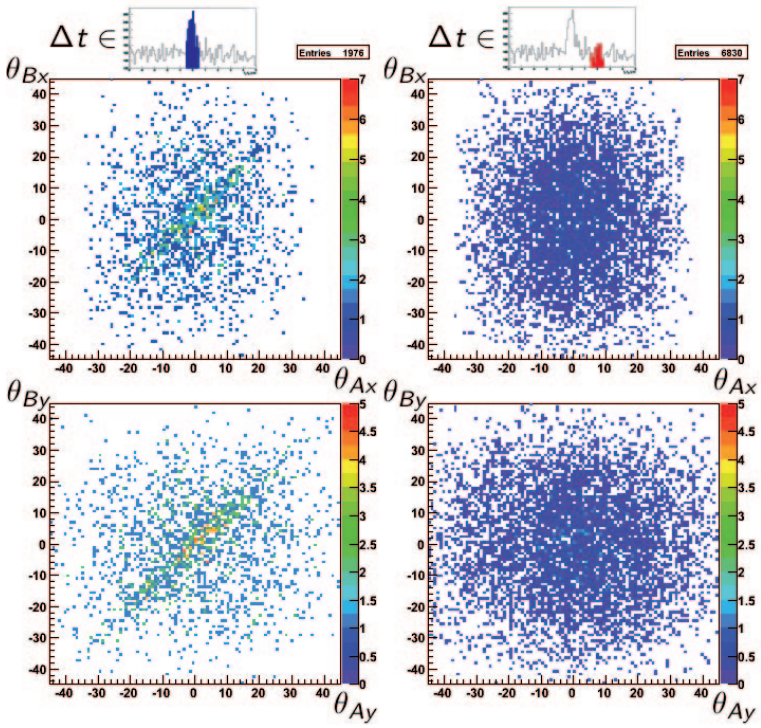

Fig. 7. – Left: angular distribution of the coincident muon pairs in two orthogonal directions, x (up) and y (down), in a common reference frame for the two stations A and B. Right: same plot for independent muon pairs, namely, muon pairs detected at the two stations far away from the temporal coincidence window.

We can better analyze the discovered angular correlation by exploiting the temporal correlation between the detected cosmic ray muons. To this end we define a coincidence time window centered around $\Delta t = 0$ and having total width approximately equal to the peak base (*i.e.*, $4\sigma \approx 900\,\text{ns}$); this enables us to compare the angular distribution of coincident muon pairs with the angular distribution of independent muon pairs (*i.e.*, muons detected outside the coincidence window). In fig. 7 we plot the angular distribution of the coincident muon pairs, by defining θ_A and θ_B as the detection angles at station A and B, respectively, with respect to the vertical direction; a common reference frame (x, y) has been defined for the two stations in a plane parallel to the MRPCs. The angular correlation (as opposed to anti-correlation) gives rise to the distribution of the coincident muon pairs around the diagonal (as opposed to the anti-diagonal) of the $(\theta_{Ai}, \theta_{Bi})$-planes, with $i = x, y$, as clearly appears from the two plots in the left column of fig. 7. The symmetric distribution of muon pairs detected outside the coincidence window (right column in fig. 7) indicates that independent muon pairs are neither correlated nor anti-correlated; the angular correlation characterizing coincident muon pairs is thus a pure second order effect (*i.e.*, it is not a trivial projection of the angular distribution of independent muon pairs).

Let us now exploit the angular correlation to perform the first feasibility study of ghost imaging with cosmic ray muons. As schematically represented in fig. 8, we simulate the

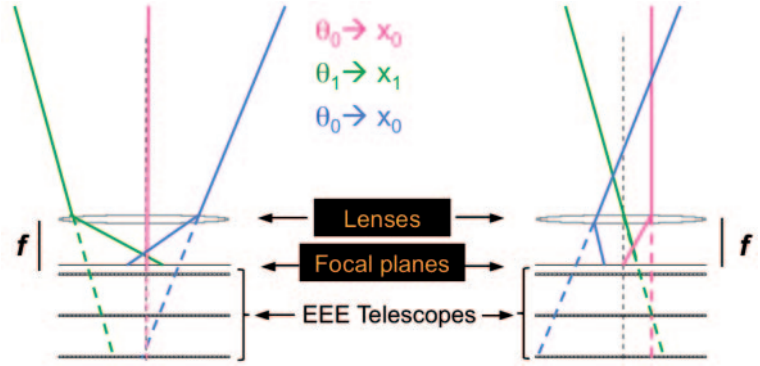

Fig. 8. – The presence of a lens of focal length f is simulated on top of each telescope: All detected muons coming at a given angle are collected in a given point of the focal plane, independent of their position of incidence. The dashed line is the reconstructed track of detected muons; the continuous line is the track due to the simulated lens.

presence of a lens on top of each telescope; this enables studying the position-position correlation between the focal planes of the two lenses, similar to the optical set-up of fig. 2. The possibility of simulating the presence of the two lenses comes from the availability of the detected muon tracks, as made possible by EEE telescopes. The reconstructed muon tracks give the angular information required for simulating the deviation a muon would experience if a lens is placed along its path. In fact, as depicted in fig. 8, independently of the incidence positions of the detected muons, their positions in the focal planes of the simulated lenses is: $x_{A,B} = f \tan(\theta_{A,B})$, where f is the focal length of both simulated lenses, and $\theta_{A,B}$ is the incidence angle of muons detected at station A and B, respectively. In fig. 9 we plot the results obtained by simulating two lenses of focal length $f = 10\,\mathrm{cm}$; the spatial distribution of both coincident (blu) and independent (red) muon pairs is shown as a function of their relative distance $|\boldsymbol{\rho}_A - \boldsymbol{\rho}_B|$ in the focal planes of the two simulated lenses.

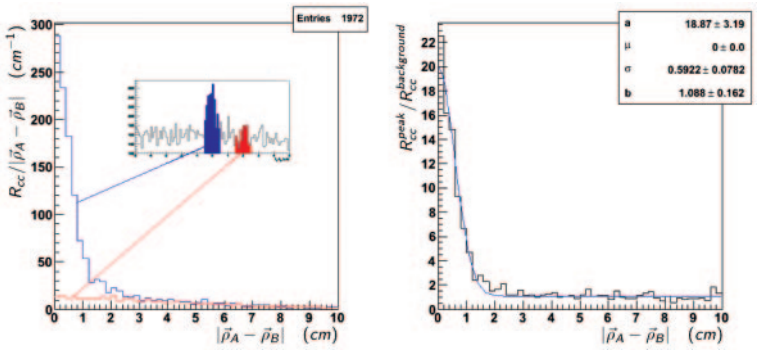

Fig. 9. – (Colour on-line) Left: spatial distribution of both coincident muon pairs (blue) and independent muons (red) as a function of their relative distance $|\boldsymbol{\rho}_A - \boldsymbol{\rho}_B|$ in the focal planes of the two simulated lenses ($f = 10\,\mathrm{cm}$). Right: normalized spatial distribution of muon pairs detected in coincidence; the continuous curve is the Gaussian fit.

The high-visibility peak characterizing muon pairs detected in coincidence indicates that the angular correlation is naturally transformed into a position-position correlation between the focal planes of two lenses. In order to quantify such position-position correlation we normalize the distribution of the coincident muon pairs with respect to the distribution of the independent pairs, by dividing the blue by the red curve, and evaluate the width of the resulting distribution by performing a Gaussian fit, as shown in fig. 9. The spatial correlation peak has 90% visibility and 0.6 cm width, corresponding to an angular correlation of 3.6° (in agreement with the analysis performed without lenses). This peak represents the point-spread-function of a muon ghost imaging scheme analogous to the classical version of optical ghost imaging (fig. 2). We are currently working on the simulation of the remaining two optical ghost imaging protocols, as shown in figs. 1 and 3.

We are also extending the present analysis to both energy and momentum; in fact, real objects will have the potentials to be "ghostly imaged" by means of cosmic ray muons only if the strong angular correlation exploited so far is accompanied by energy correlation, thus resulting in sufficient momentum-momentum correlation between muon pairs detected in coincidence in two distant locations.

5. – Conclusion

After reviewing the basic principles of optical ghost imaging, we have presented our recent progresses concerning the feasibility study of ghost imaging with massive particles. In particular, we have considered cosmic ray muons detected in L'Aquila within the EEE project [12]. Such preliminary analysis has the potentials to pave the way toward the extension to massive particles of many other intriguing quantum-optical phenomena involving classical and non-classical correlations.

Our present efforts aim at investigating the potentialities of cosmic ray muons for long-distance remote-sensing applications, while gaining a deeper comprehension of the correlations characterizing this naturally available source of massive particles.

* * *

The author sincerely thanks all co-authors of this work: F. Di Lena, M. D'Incecco, A. Garuccio, R. Moro, A. Regano, F. Romano, and G. Scarcelli, who have actively contributed to the entire work presented in this paper. A special thank to the EEE collaboration and the "Centro Studi e Ricerche E. Fermi", for giving us permission to analyze the data taken in L'Aquila within the EEE project; the availability of these data has been essential for conducting the present feasibility study. The author is particularly thankful to M. Abbrescia for interesting insights about the working principle of the EEE telescopes and the general setup of the EEE experiment, particularly useful in the start-up phase of the present research.

REFERENCES

[1] Belinskii and Klyshko, *JETP*, **105** (1994) 487; Klyshko D. N., *Sov. Phys. Usp.*, **31** (1988) 74.
[2] Pittman T. B., Shih Y. H., Strekalov D. V. and Sergienko A. V., *Phys. Rev. A*, **52** (1995) R3429.
[3] Gatti A. *et al.*, *Phys. Rev. A*, **70** (2004) 013802.

[4] Valencia A., Scarcelli G., D'Angelo M. and Shih Y., *Phys. Rev. Lett.*, **94** (2005) 063601.
[5] Meyers R. *et al.*, *Phys. Rev. A*, **77** (2008) 041801.
[6] Scarcelli G., *Nat. Phys.*, **5** (2009) 252.
[7] Brida G., Genovese M. and Ruo Berchera I., *Nat. Photon.*, **4** (2010) 227.
[8] Zichichi A., *La Scienza nelle Scuole, EEE-Extreme Energy Events*, presented in Bologna, 1 Aprile 2005; also at `http://www.centrofermi.it/attachments/article/10/EEE.pdf` and `www.centrofermi.it/eee`.
[9] Akindinov A. *et al.*, *Nucl. Instrum. Methods A*, **456** (2000) 16.
[10] Abbrescia M. *et al.*, *Nucl. Instrum. Methods A*, **593** (2008) 263.
[11] Regano A. *et al.*, oral presentation at XCV Congresso Nazionale, Società Italiana di Fisica (SIF), Bari (2009).
[12] Abbrescia M. *et al.*, *Nuovo Cimento B*, **125** (2010) 243.
[13] D'Angelo M., Kim Y. H., Kulik S. P. and Shih Y. H., *Phys. Rev. Lett.*, **92** (2004) 233601.
[14] D'Angelo M., Valencia A., Rubin M. H. and Shih Y. H., *Phys. Rev. A*, **72** (2005) 013810.
[15] Bennink R. S., Bentley S. J., Boyd R. W. and Howell J. C., *Phys. Rev. Lett.*, **92** (2004) 033601.
[16] Howell J. C., Bennink R. S., Bentley S. J. and Boyd R. W., *Phys. Rev. Lett.*, **92** (2004) 210403.
[17] Bennink R. S., Bentley S. J. and Boyd R. W., *Phys. Rev. Lett.*, **89** (2002) 113601.
[18] Ferri F. *et al.*, *Phys. Rev. Lett.*, **94** (2005) 183602; Zhang *et al.*, *Opt. Lett.*, **30** (2005) 2354.
[19] Scarcelli G., Valencia A. and Shih Y., *Europhys. Lett.*, **68** (2004) 618.
[20] D'Angelo M. and Shih Y. H., *Laser Phys. Lett.*, **2** (2005) 567.
[21] Scarcelli G., Berardi V. and Shih Y., *Phys. Rev. Lett.*, **96** (2006) 063602.
[22] Scarcelli G., Berardi V. and Shih Y., *Appl. Phys. Lett.*, **88** (2006) 061106.
[23] Di Lena F., Laurea Thesis in Physics, Università degli Studi di Bari (2011).
[24] Klyshko D. N., *Photon and Nonlinear Optics*, (Gordon and Breach Science, New York) 1988.
[25] Gatti A., Brambilla E. and Lugiato L. A., *Phys. Rev. Lett.*, **90** (2003) 133603.
[26] Hanbury-Brown R., *Intensity Interferometer*, (Taylor and Francis Ltd, London) 1974; Hanbury-Brown R. and Twiss R. Q., *Nature*, **177** (1956) 27; **178** (1956) 1046.
[27] Migdall A., *Phys. Today*, **52** (issue 1) (1999) 41.
[28] Abbrescia M. *et al.*, *Nucl. Phys. B, Proc. Suppl.*, **190** (2009) 38.